Processes involving electron capture and multiple ionization in collisions of fast H^+ and He^{2+} ions with lead atoms

P. C. E. McCartney, M. B. Shah, J. Geddes, and H. B. Gilbody
Department of Pure and Applied Physics, The Queen's University of Belfast, Belfast, United Kingdom
(Received 25 May 1999)

A crossed-beam technique incorporating time-of-flight analysis and coincidence counting of the collision products has been used to study Pb^{q+} formation with q up to 8 in collisions between ground-state Pb atoms and H^+ and He^{2+} ions within the range 50–600 keV amu^{-1}. The separate cross sections for simple charge transfer, transfer ionization, and pure ionization leading to the formation of Pb^{q+} ions have been obtained and the relative importance of these processes has been established. Accurate measurements and rigorous theoretical descriptions of these multielectron processes in such heavy atoms are difficult and data are still very limited. The present measurements have been designed to extend our previous studies of multiple ionization of a few selected heavy metal atoms and to provide a further check on the extent to which the main collision processes can be described quantitatively in terms of simple models based on an independent electron description. In our previous work with Fe, Cu, and Ga atoms using the same experimental approach, we were able to describe the formation of multiply charged ions through both transfer ionization and pure ionization with a high degree of success using an independent electron model. However, the present results for Pb show that the success of this simple approach is much more limited for these much heavier atoms. [S1050-2947(99)00412-6]

PACS number(s): 34.50.Fa

I. INTRODUCTION

There is strong current interest in many-electron collision processes (cf. Shevelko and Tawara [1]). Apart from the need to obtain a better fundamental understanding, reliable data on processes involving multiple ionization of a wide range of heavy atom species are important for the accurate modeling of fusion plasmas (cf. Janev [2]) and in astrophysical situations.

In previous work in this laboratory [3–9], we have used a crossed-beam technique incorporating time-of-flight analysis and coincidence counting of the collision products to obtain the separate cross sections for both electron capture and ionization leading to n-fold ionized product ions in collisions of fast H^+ and He^{2+} ions with a few heavy metal species. Measurements of this type are complex and difficult and, for this reason, we have concentrated on a few selected target species and tried to establish to what extent processes leading to multiple ionization can be described in terms of simple models based upon an independent electron description (cf., McGuire [10]). Previously we have studied collisions of H^+ and He^{2+} ions with ground-state $3p^6 3d^6 4s^2\ ^5D_4$Fe, $3p^6 3d^{10} 4s\ ^2S_{1/2}$, Cu, and $3p^6 3d^{10} 4s^2 4p\ ^2P_{1/2}$ Ga atoms within the energy range 38–1440 keV amu^{-1}, and the different electronic configurations of these targets have provided interesting tests of our simple theoretical models.

In the case of H^+ impact, cross sections ${}_{10}\sigma_{0q}$ for the one-electron capture process

$$H^+ + X \rightarrow H + X^{q+} + (q-1)e \tag{1}$$

for $q=1-4$ for Fe, $q=1-5$ for Cu, and $q=1-5$ for Ga were determined. In Eq. (1), $q=1$ corresponds to simple charge transfer while $q>1$ corresponds to transfer ionization where one-electron capture takes place simultaneously with multiple ionization of the target. In the case of He^{2+} impact, the corresponding cross sections ${}_{20}\sigma_{1q}$ for one-electron capture and ${}_{20}\sigma_{0q}$ for two-electron capture leading to X^{q+} products with q up to 7 were determined. Cross sections for the pure ionization processes

$$H^+ + X \rightarrow H^+ + X^{q+} + qe \tag{2}$$

with $q=1-5$ and

$$He^{2+} + X \rightarrow He^{2+} + X^{q+} + qe \tag{3}$$

with $q=1-3$ were also determined.

In our attempts to obtain a simple theoretical description of our previous electron capture and ionization data for Fe and Cu, we assumed that electron removal takes place primarily from the outer $4s$ and $3d$ subshells. We were then able to describe our measurements quantitatively in terms of an independent-electron model with a high degree of success. In the case of Ga, our model was modified to also take account of electron removal from the weakly bound $4p$ subshell and the fact that removal of a $3d$ electron leads to Ga^{2+} formation through autoionization. This modified model was also shown to provide a reasonable description of the formation of Ga^{q+} ions but with much greater success for H^+ than for He^{2+} ion impact.

In the present work, in order to carry out further tests of our simple theoretical model, we have carried out similar measurements of electron capture and ionization in collisions of H^+ and He^{2+} ions with ground-state $5d^{10} 6s^2 6p^2\ ^3P_0$ Pb atoms within the range 50–600 keV amu^{-1} for processes leading to Pb^{q+} formation with q up to 8. The electron subshell structure of Pb is significantly different from the heavy-metal atoms considered previously, and the present studies of this much more complex system provide further insight into the limitations of our simple descriptions of multiple ionization based on an independent-electron model.

TABLE I. Cross sections ${}_{10}\sigma_{0q}$ for one-electron capture in H^+-Pb collisions leading to the formation of Pb^{q+} ions. Total cross sections $\sigma_{10}=\Sigma_{10}\sigma_{0q}$ are also shown.

Energy (keV amu^{-1})	σ_{10} (10^{-17} cm^2)	${}_{10}\sigma_{01}$ (10^{-18} cm^2)	${}_{10}\sigma_{02}$ (10^{-17} cm^2)	${}_{10}\sigma_{03}$ (10^{-17} cm^2)	${}_{10}\sigma_{04}$ (10^{-18} cm^2)	${}_{10}\sigma_{05}$ (10^{-19} cm^2)	${}_{10}\sigma_{06}$ (10^{-19} cm^2)
83.5	23.4±1.27	34.0±5.4	15.7±1.1	2.94±0.29	14.1±1.9		
100	21.6±1.18	22.1±3.1	14.8±1.1	3.67±0.26	8.73±1.19		
120	10.9±0.64	7.29±1.0	7.31±0.59	2.25±0.22	6.14±0.72	3.7±1.7	
145	10.4±0.58	3.71±0.72	6.87±0.53	2.25±0.20	8.13±0.68	9.4±3.2	
175	6.47±0.30	1.71±0.36	3.93±0.25	1.56±0.13	6.30±0.66	11.8±2.6	5.98±3.50
210	5.70±0.25	1.68±0.37	3.32±0.22	1.43±0.10	5.80±0.56	19.1±2.4	1.48±0.90
250	3.87±0.16	0.80±0.17	2.19±0.13	1.04±0.08	4.46±0.48	10.8±1.4	
300	2.60±0.10	0.37±0.08	1.42±0.07	0.72±0.07	3.00±0.30	9.30±1.12	2.8±1.4
360	1.47±0.06	0.29±0.06	0.76±0.05	0.44±0.03	1.77±0.20	4.60±0.62	2.4±1.5
430	0.75±0.04	0.14±0.04	0.39±0.03	0.23±0.02	0.74±0.08	2.03±0.22	2.4±1.9
500	0.40±0.02		0.20±0.01	0.13±0.01	0.48±0.05	1.45±0.21	
600	0.21±0.02	0.08±0.05	0.08±0.01	0.07±0.01	0.39±0.03	1.13±0.11	

II. EXPERIMENTAL APPROACH

The apparatus, measurement, and normalization procedure was similar to that used in our previous measurements (cf., Patton *et al.* [4] and Shah *et al.* [7]), so that only the essential features need to be summarized here.

A primary beam of momentum analyzed H^+ or He^{2+} ions of selected energy within the range 50–600 keV amu^{-1} was arranged to intersect (at right angles) in a high vacuum region a thermal energy beam of ground-state Pb atoms derived from an oven source [11]. The slow Pb^{q+} ions and electrons formed as collision products in the crossed-beam region were extracted with high efficiency by a transverse electric field applied between two high transparency grids and, after further acceleration through a potential difference of 4.5 kV, were separately counted by particle multipliers. Pb^{q+} ions in any particular charge state q were selectively identified and distinguished from background gas collision products by time-of-flight analysis. As in our earlier work, signals S_q corresponding to the Pb^{q+} yields per unit primary ion current were recorded as the potential difference through which the ions were accelerated was increased from 3 to 6 kV. It was then found that the signal ratios S_q/S_1 became constant above 4.5 kV, indicating that the counting efficiency was essentially independent of q within an estimated uncertainty of 7%.

The Pb^{q+} ions arising from electron capture collisions could be identified by counting them in coincidence with the fast H atoms, He^+ ions, or He atoms arising from the same events. The latter were recorded (after charge analysis by electrostatic deflection) by a third-particle multiplier located beyond the crossed-beam region. The Pb^{q+} ions arising from both transfer ionization and pure ionization could be identi-

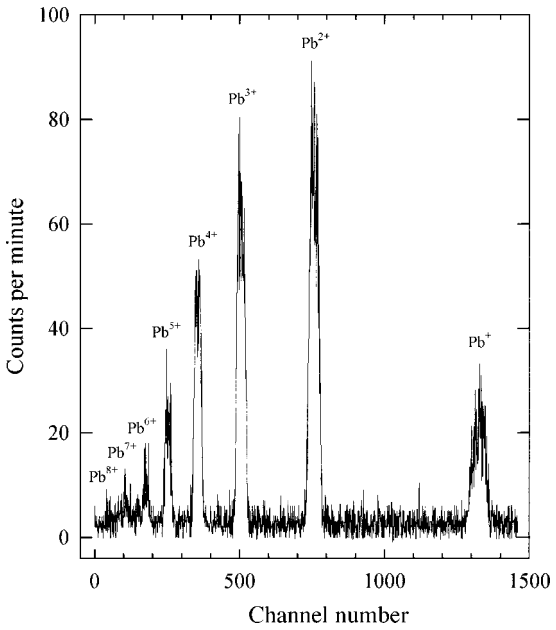

FIG. 1. Fast He^+/slow Pb^{q+} ion time-of-flight coincidence spectrum resulting from one-electron capture by 290 keV He^{2+} ions in collisions with Pb atoms. Adjacent channel separation is 2 ns.

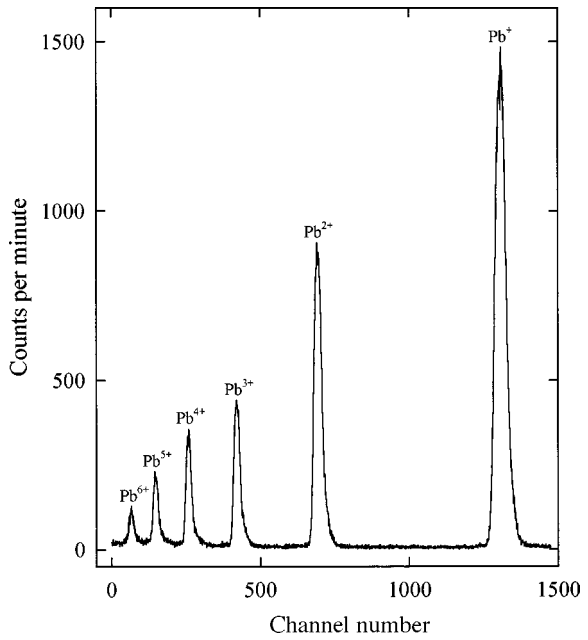

FIG. 2. Slow Pb^{q+}/electron time-of-flight coincidence spectrum resulting from ionization of Pb atoms by 150 keV He^{2+} ions. Adjacent channel separation is 2 ns.

TABLE II. Cross sections ${}_{20}\sigma_{1q}$ for one-electron capture in He^{2+}-Pb collisions leading to the formation of Pb^{q+} ions. Total cross sections $\sigma_{21}=\Sigma_{20}\sigma_{1q}$ are also shown.

Energy (keV amu^{-1})	σ_{21} (10^{-16} cm^2)	${}_{20}\sigma_{11}$ (10^{-17} cm^2)	${}_{20}\sigma_{12}$ (10^{-16} cm^2)	${}_{20}\sigma_{13}$ (10^{-16} cm^2)	${}_{20}\sigma_{14}$ (10^{-16} cm^2)	${}_{20}\sigma_{15}$ (10^{-17} cm^2)	${}_{20}\sigma_{16}$ (10^{-17} cm^2)	${}_{20}\sigma_{17}$ (10^{-18} cm^2)	${}_{20}\sigma_{18}$ (10^{-18} cm^2)
50	24.4±1.0	67.7±4.1	8.97±0.59	4.96±0.52	2.72±0.34	8.51±1.28	1.35±0.31		
60	16.2±0.7	33.6±2.7	5.90±0.41	3.77±0.39	2.19±0.28	8.21±1.20	1.79±0.38	1.74±0.73	
72.5	13.9±0.6	19.4±1.7	4.88±0.37	3.62±0.36	2.28±0.29	8.85±1.29	2.47±0.50	7.19±2.91	
87.5	12.0±0.5	9.95±0.98	4.05±0.31	3.37±0.32	2.22±0.25	9.84±1.35	3.15±0.59	5.37±2.18	0.23±0.22
105	9.88±0.46	4.24±0.44	3.13±0.24	2.91±0.28	1.97±0.22	9.87±1.33	3.59±0.63	8.97±2.93	1.29±0.77
125	8.56±0.37	1.96±0.24	2.54±0.18	2.44±0.21	1.80±0.19	9.76±1.32	4.16±0.66	14.3±2.93	4.50±3.24
150	6.96±0.31	0.68±0.09	1.97±0.17	1.95±0.17	1.54±0.15	8.66±0.95	4.01±0.67	13.8±2.62	2.41±0.90
180	5.56±0.29	0.41±0.06	1.46±0.12	1.54±0.15	1.24±0.14	7.79±1.48	3.63±0.53	11.8±2.42	1.95±0.67
215	4.46±0.21	0.25±0.04	1.10±0.09	1.19±0.12	1.04±0.12	6.55±0.75	3.06±0.42	10.7±2.19	2.61±0.85
250	3.45±0.16	0.24±0.05	0.81±0.07	0.92±0.09	0.83±0.08	5.30±0.56	2.35±0.37	8.02±1.57	2.25±0.90
300	2.47±0.11	0.13±0.06	0.56±0.05	0.66±0.07	0.60±0.05	3.82±0.42	1.68±0.21	6.55±1.24	2.32±0.67
360	2.02±0.09	0.06±0.03	0.46±0.04	0.54±0.05	0.50±0.05	3.18±0.36	1.37±0.25	5.03±0.90	1.70±0.56

fied by counting them in coincidence with the electrons arising from the same events. Alternatively the primary ion beam could be pulsed and the Pb^{q+} product ions extracted from the crossed-beam region by a delayed extraction pulse of about 70 V cm^{-1} prior to identification by time-of-flight analysis. Typical Pb^{q+}-fast-ion/atom and Pb^{q+}-electron time-of-flight coincidence spectra are shown in Figs. 1 and 2. A careful analysis of spectra of this type, in the way described previously [4, 7], allowed determination of the separate cross sections ${}_{10}\sigma_{0q}$ for one-electron capture by 83.5–600 keV amu^{-1} H^+ ions where $q=1-6$, ${}_{20}\sigma_{1q}$, for one-electron capture by 50–360 keV amu^{-1} He^{2+} ions where $q=1-8$, and ${}_{20}\sigma_{0q}$ for two-electron capture by 50–250 keV amu^{-1} He^{2+} ions where $q=2-7$. In addition, the pure ionization cross sections ${}_{10}\sigma_{1q}$ for 100–600 keV amu^{-1} H^+ ions, where $q=1-6$, and ${}_{20}\sigma_{2q}$ for 50–350 keV amu^{-1} He^{2+} ions, where $q=1-5$, were determined. It should be noted that, while the e-Pb^+ coincidence signals allowed the pure single ionization cross sections to be determined directly, for $q\geq 2$ the analysis was complicated by contributions from transfer ionization. In this case, as in our previous work, we pulsed the primary ion beam and first obtained the total cross sections for Pb^{q+} formation. Subtraction of the transfer ionization contributions then allowed the individual pure ionization cross sections to be determined.

Our measured relative cross sections were normalized to our recently measured cross sections [12] for ionization of Pb by electron impact. This normalization procedure, which has been described in detail previously [13], involved the careful substitution of a pulsed primary ion beam by a pulsed beam of electrons while the target conditions remained unchanged.

III. RESULTS FOR MULTIPLE IONIZATION BY ELECTRON CAPTURE

Cross sections ${}_{10}\sigma_{0q}$ and ${}_{20}\sigma_{1q}$ for one-electron capture by H^+ and He^{2+} leading to Pb^{q+} formation are shown in Tables I and II while cross sections ${}_{20}\sigma_{0q}$ for two-electron capture by He^{2+} ions are shown in Table III. Total cross sections $\sigma_{10}\approx\Sigma_{q=1}^{q=6}\,{}_{10}\sigma_{0q}$ and $\sigma_{21}\approx\Sigma_{q=1}^{q=8}\,{}_{20}\sigma_{1q}$ for one-electron capture and $\sigma_{20}\approx\Sigma_{q=2}^{q=7}\,{}_{20}\sigma_{0q}$ for two-electron capture are also included. The uncertainties associated with individual cross sections reflect 67% confidence levels based upon the degree of reproducibility of the measured values. In addition, all cross sections are subject to estimated uncertainties of 12% in absolute value as a result of the normalization

TABLE III. Cross sections ${}_{20}\sigma_{0q}$ for two-electron capture in He^{2+}-Pb collisions leading to the formation of Pb^{q+} ions. Total cross sections $\sigma_{20}=\Sigma_{20}\sigma_{0q}$ are also shown.

Energy (keV amu^{-1})	σ_{20} (10^{-16} cm^2)	${}_{20}\sigma_{02}$ (10^{-18} cm^2)	${}_{20}\sigma_{03}$ (10^{-17} cm^2)	${}_{20}\sigma_{04}$ (10^{-17} cm^2)	${}_{20}\sigma_{05}$ (10^{-17} cm^2)	${}_{20}\sigma_{06}$ (10^{-17} cm^2)	${}_{20}\sigma_{07}$ (10^{-18} cm^2)
50	3.73±0.21	17.8±3.54	11.7±1.04	14.7±1.56	6.36±0.80	1.95±0.29	8.25±1.69
60	3.05±0.18	9.42±1.74	9.12±0.96	12.1±1.32	5.75±0.72	1.77±0.26	8.44±1.72
72.5	2.40±0.13	6.20±1.08	6.58±0.62	9.42±0.95	4.84±0.56	1.69±0.23	8.32±1.65
87.5	2.01±0.10	4.69±0.75	5.22±0.49	7.42±0.69	4.31±0.48	1.74±0.24	8.97±1.70
105	1.66±0.08		4.16±0.44	5.79±0.52	3.93±0.39	1.80±0.23	8.85±1.47
125	1.42±0.08		3.26±0.32	4.80±0.54	3.47±0.36	1.82±0.23	8.47±1.24
150	1.17±0.06		2.44±0.25	3.58±0.36	3.03±0.31	1.77±0.24	8.32±1.32
180	0.90±0.04		1.67±0.13	2.66±0.24	2.50±0.22	1.47±0.16	7.19±1.05
212.5	0.66±0.03		1.20±0.12	1.77±0.16	1.88±0.13	1.13±0.14	5.94±0.85
250	0.48±0.03		0.87±0.09	1.29±0.14	1.29±0.10	0.90±0.10	4.58±0.72

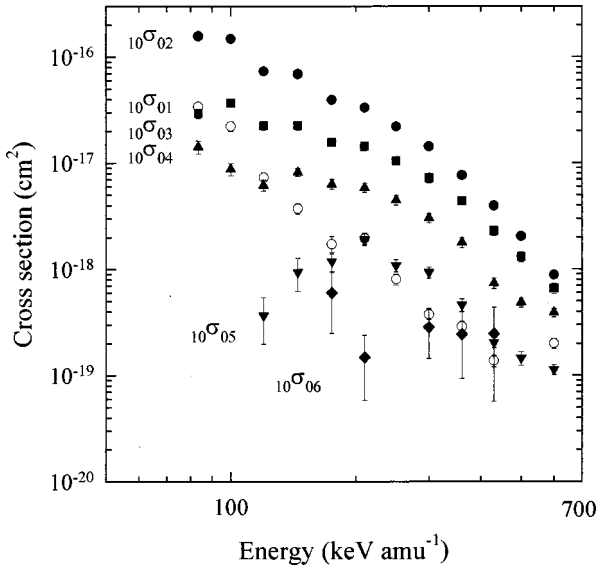

FIG. 3. Cross sections $_{10}\sigma_{0q}$ for one-electron capture by H^+ ions in collisions with Pb atoms leading to Pb^{q+} formation.

to our previously measured electron impact cross sections [12].

Figure 3 shows cross sections $_{10}\sigma_{0q}$ for one-electron capture by H^+ ions leading to Pb^{q+} ions where $q=1-6$. Over the energy range shown, cross sections $_{10}\sigma_{02}$ for transfer ionization leading to Pb^{2+} formation can be seen to greatly exceed the simple charge-transfer cross sections $_{10}\sigma_{01}$ and provide the dominant contribution to the total one-electron capture cross section σ_{10}. Values of $_{10}\sigma_{0q}$ for $q>2$ can also be seen to progressively exceed $_{10}\sigma_{01}$ as the impact energy increases. As q increases, a high-energy ''bulge'' in the cross-section curves $_{10}\sigma_{0q}$ can be seen to become more pronounced and, for $q=5$ and 6, the curves exhibit maxima.

Figure 4 shows cross sections $_{20}\sigma_{1q}$ for one-electron capture by He^{2+} ions. As in the case of H^+ impact, the simple charge-transfer contribution $_{20}\sigma_{11}$ to the total one-electron capture cross section decreases rapidly with increasing energy and is progressively exceeded by the transfer ionization

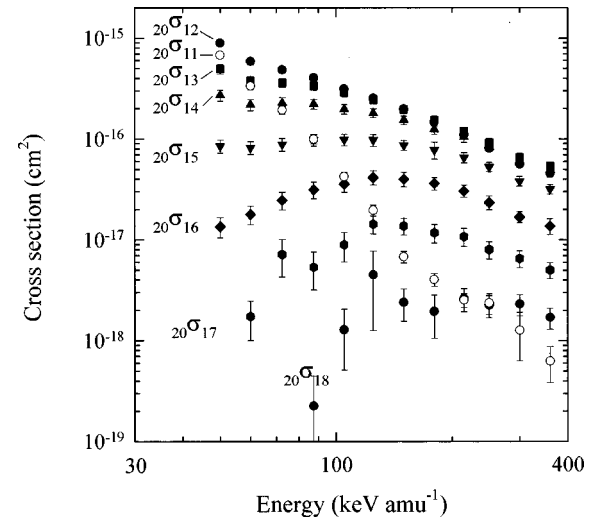

FIG. 4. Cross sections $_{20}\sigma_{1q}$ for one-electron capture by He^{2+} ions in collisions with Pb atoms leading to Pb^{q+} formation.

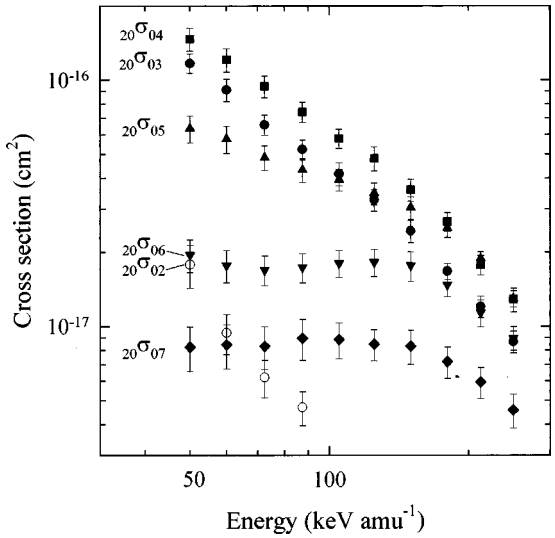

FIG. 5. Cross sections $_{20}\sigma_{0q}$ for two-electron capture by He^{2+} ions in collisions with Pb atoms leading to Pb^{q+} formation.

contributions $_{20}\sigma_{1q}$ for $q>1$ at higher energies as q increases. Again, high-energy ''bulges'' in the cross-section curves $_{20}\sigma_{1q}$ become broad maxima with increasing q. In the case of two-electron capture, the simple charge-transfer cross section $_{20}\sigma_{02}$ again decreases rapidly with increasing energy (Fig. 5) and is exceeded by the transfer ionization cross sections $_{20}\sigma_{0q}$ for $q=3-6$ over the energy range considered. The contribution from $_{20}\sigma_{04}$ is actually dominant over most of the energy range considered. In addition, at energies above about 60 keV amu^{-1}, even values of $_{20}\sigma_{17}$ leading to Pb^{7+} greatly exceed $_{20}\sigma_{02}$. Very flat maxima are apparent in the $_{20}\sigma_{06}$ and $_{20}\sigma_{07}$ cross-section curves. It is worth noting that two-electron capture into excited states of the projectile which then decay rapidly can effectively provide contributions to our measured one-electron capture cross sections. However, our experimental technique is unable to quantitatively assess such contributions.

In all the transfer ionization processes, electron capture is accompanied by the removal of additional electrons from the outer subshells, the energy for which can be provided through binary-type collisions. Figures 6 and 7 show the energy dependence of our measured charge-state fractions F_q for Pb^{q+} ions formed in one-electron capture by H^+ and He^{2+} ions, respectively. At impact energies below the present low-energy limit, simple charge transfer (corresponding to $q=1$) will involve the capture of weakly bound outer-shell electrons. However, in the present energy range, capture of the more tightly bound $6s$, $5d$, and even $5p$ electrons would be expected to become significant. As in our previous measurements on Ga [9], the creation of an electron vacancy in an inner shell of Pb can also lead to the formation of Pb^{2+} ions as a result of autoionization. This process can result in a reduction in F_1 and an enhancement of F_2 leading to values which are only weakly dependent on impact energy. This is in accord with our results shown in Fig. 6 for H^+ impact, where $F_2>F_1$ over the entire energy range, and in Figure 7 for He^{2+} impact, where $F_2>F_1$ over most of the energy range. Similar enhancements of F_q for higher values of q are possible and evidence of this is provided by the enhancements of multiple ionization in Pb by autoionization ob-

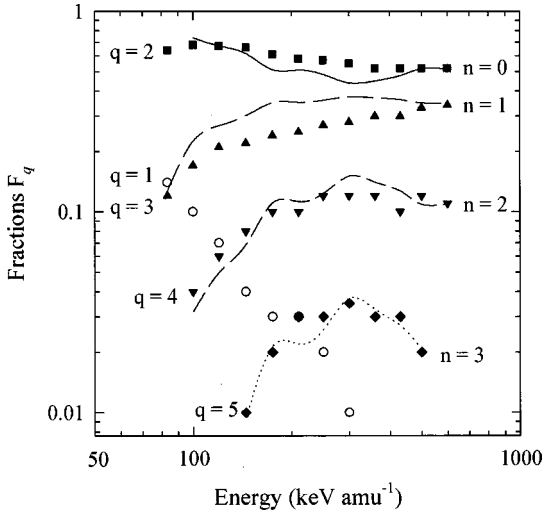

FIG. 6. Measured charge-state fractions F_q (shown as data points) for Pb^{q+} ions formed by one-electron capture in single collisions between H^+ ions and ground-state Pb atoms. Curves show calculated ionization probabilities P_n, where $n=(q-2)$ (see text) based on binomial distributions.

served in our recent electron-impact measurements [12].

In our previous studies [6,8,9] of electron capture in Fe, Cu, and Ga, we described our observed values of F_q with a high degree of success in terms of an independent electron model in which we expressed the probability of transfer ionization as the product of the one-electron capture probability P_c and an ionization probability P_n for the removal of n additional electrons from the target. In the case of Fe and Cu, we took $n=q-1$ for $q \geqslant 1$. However, in the case of Ga, where autoionization following one-electron capture results in a dominant Ga^{2+} contribution, it was more appropriate to consider the number of electrons removed by ionization as $n=(q-2)$. We were then able to satisfactorily fit our experimental data for all values of q.

In the present case of Pb where F_2 is seen to be dominant,

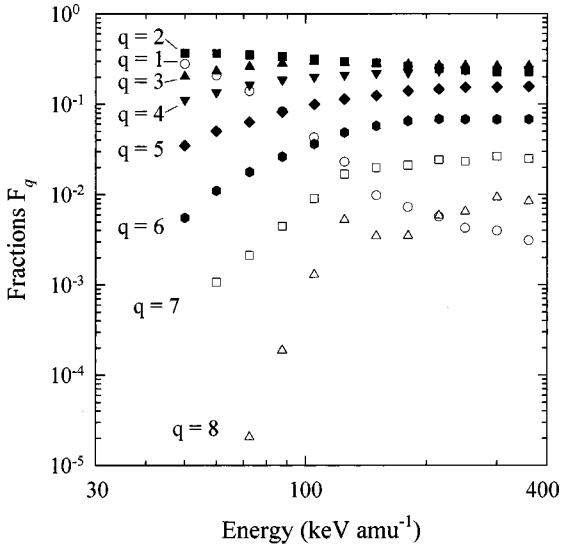

FIG. 7. Measured charge-state fractions F_q for Pb^{q+} ions formed by one-electron capture in single collisions between He^{2+} ions and ground-state Pb atoms.

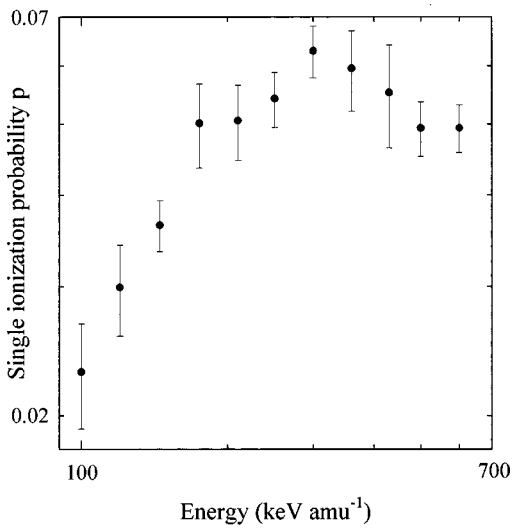

FIG. 8. Energy dependence of the single electron ionization probability p derived from the binomial fits (see text) to the measured values of F_q for one-electron capture in single H^+-Pb collisions.

as in the case of Ga we take $n=q-2$. We can then use an analysis similar to that used previously in which the cross section ${}_{10}\sigma_{01}$ may be expressed as

$$ {}_{10}\sigma_{0q}=2\pi\int_0^\infty bP_c(b)P_n(b)db, \tag{4}$$

where b is the impact parameter. Assuming $P_n(b)$ to be constant over the relatively small range of impact parameters where electron capture occurs, then

$$ P_n={}_{10}\sigma_{0q}\sigma_{10}, \tag{5}$$

where the total electron capture cross section $\sigma_{10}=\Sigma_q {}_{10}\sigma_{0q}$. Measured values of F_q can then be identified with P_n through Eq. (5).

The probability P_n that n electrons are ejected from either the $5d$, $6s$, or $6p$ subshells can be estimated as detailed in our previous work [6] on the basis of binomial distributions

$$ P_n=(N!/n!(N-n)!)p^n(1-p)^{(N-n)}, \tag{6}$$

where p is the single electron ionization probability and N is the total number of electrons available for ionization, which is 13 in this case for the $5d$, $6s$, and $6p$ subshells we consider. We assume that the probability for electron removal is the same for each subshell and that the time for autoionization following one-electron capture is longer than the interaction time of the fast projectile ion. We have fitted the values of P_n obtained in this way to experimental values of F_q using the weighted least-squares method, and the results for H^+ impact are included in Fig. 6, while the corresponding values of the single electron ionization probability p derived from the binomial fits to measured values of F_q are shown in Fig. 8.

In Fig. 6 it can be seen that our model provides a reasonably good quantitative description of our observed fractions F_2, F_3, F_4, and F_5 in one-electron capture by H^+ impact, especially for the higher q values. However, the fitting pro-

TABLE IV. Cross sections $_{10}\sigma_{1q}$ for pure ionization in H^+-Pb collisions leading to the formation of Pb^{q+} ions.

Energy (keV amu^{-1})	$_{10}\sigma_{11}$ (10^{-16} cm^2)	$_{10}\sigma_{12}$ (10^{-16} cm^2)	$_{10}\sigma_{13}$ (10^{-17} cm^2)	$_{10}\sigma_{14}$ (10^{-17} cm^2)	$_{10}\sigma_{15}$ (10^{-18} cm^2)	$_{10}\sigma_{16}$ (10^{-18} cm^2)
100	8.16±0.82	2.78±0.38	4.04±1.69			
120	8.01±0.80	3.58±0.36	7.78±1.67			
145	6.86±0.65	3.27±0.34	6.20±1.54	1.35±0.27		
175	6.55±0.58	3.61±0.31	8.67±1.24	1.89±0.33		
210	5.83±0.50	3.24±0.26	7.34±0.88	2.16±0.34		
250	5.19±0.45	3.42±0.25	8.54±0.81	2.64±0.34		
300	4.65±0.38	2.89±0.25	6.73±0.76	2.25±0.34	5.4±2.2	1.57±0.79
360	3.77±0.36	2.72±0.24	6.30±0.69	2.10±0.34	5.5±1.1	1.13±0.45
430	3.46±0.33	2.42±0.23	5.61±0.57	1.85±0.33	5.09±0.76	1.17±0.43
500	3.05±0.31	2.40±0.23	5.51±0.52	1.77±0.32	4.90±0.74	1.40±0.42
600	2.65±0.29	2.20±0.22	4.98±0.52	1.60±0.32	3.56±0.54	0.94±0.28

cedure is less satisfactory than in the case of the lighter atoms Fe, Cu, and Ga considered in our previous work, probably because our attempt to allow for possible autoionization pathways is oversimplified. Increasing the pool of available electrons to include the $5p$ subshell did not improve the fits to the present experimental data.

In the case of one-electron capture by He^{2+} impact, measured fractions F_q were also compared with our predicted values of P_n based on the same model. However, in this case the fits we obtained were very unsatisfactory and are therefore not shown. This poor agreement may indicate that even deep inner-shell electrons are being captured leading to a cascading effect involving multiple Auger electron emissions, which are not included in our simple model.

IV. RESULTS FOR PURE IONIZATION

Cross sections $_{10}\sigma_{1q}$ and $_{20}\sigma_{2q}$ for pure ionization of Pb leading to the formation of Pb^{q+} ions are shown in Tables IV and V. The indicated uncertainties (at the 67% confidence level) reflect the degree of reproducibility of the individual cross sections. All cross sections are subject to an estimated additional uncertainty of 12% in absolute magnitude as a consequence of the normalization to our recent electron impact cross sections [12].

Cross sections $_{10}\sigma_{1q}$ for pure ionization of Pb by H^+ impact are shown in Fig. 9. While Pb^+ formation is dominant over the energy range considered, Pb^{2+} formation can be seen becoming comparable at our high-energy limit. A comparison with the corresponding electron capture cross sections $_{10}\sigma_{0q}$ shows that pure ionization provides the dominant contributions to Pb^+, Pb^{2+}, Pb^{3+}, Pb^{4+}, Pb^{5+}, and Pb^{6+} formation over the entire energy range considered and is not strongly energy dependent. Equivelocity values of $_{10}\sigma_{1q}$ can be seen to be decreasing by less than an order of magnitude as q increases. In addition, values of $_{10}\sigma_{12}$ can be seen to be approaching those for $_{10}\sigma_{11}$ at our high-energy limit, a behavior which is indicative of the important role of inner-shell electron removal and Auger ionization. In our previous measurements in Ga [9], the difference between these two cross sections was much larger.

Our measured cross sections for pure ionization of Pb by He^{2+} ions are shown in Fig. 10. A comparison with the corresponding one-electron capture cross sections (Fig. 4) at equivelocity shows that (as in the case of H^+ impact) Pb^+ formation is dominated by pure ionization with values of $_{20}\sigma_{21}$ becoming very large and passing through a flat maximum at about 80 keV amu^{-1}. Cross sections $_{20}\sigma_{22}$ for Pb^{2+} formation exhibit a fairly weak energy dependence and are

TABLE V. Cross sections $_{20}\sigma_{2q}$ for pure ionization in He^{2+}-Pb collisions leading to the formation of Pb^{q+} ions.

Energy (keV amu^{-1})	$_{20}\sigma_{21}$ (10^{-15} cm^2)	$_{20}\sigma_{22}$ (10^{-16} cm^2)	$_{20}\sigma_{23}$ (10^{-16} cm^2)	$_{20}\sigma_{24}$ (10^{-17} cm^2)	$_{20}\sigma_{25}$ (10^{-17} cm^2)
50	1.62±0.13	3.63±0.55			
60	1.93±0.15	4.39±0.66			
72.5	1.96±0.16	4.70±0.56	0.12±0.03		
87.5	1.98±0.16	5.12±0.61	0.17±0.03		
105	1.97±0.16	5.58±0.67	0.45±0.09		
125	1.89±0.15	5.74±0.63	0.64±0.12		
150	1.79±0.14	5.86±0.65	0.95±0.16	2.34±0.59	0.64±0.20
180	1.66±0.15	5.91±0.59	1.20±0.19	4.30±0.95	1.33±0.43
215	1.49±0.12	5.70±0.60	1.31±0.20	5.11±1.13	1.64±0.50
250	1.39±0.11	5.72±0.60	1.41±0.21	6.13±1.32	2.43±0.70
300	1.26±0.10	5.62±0.52	1.61±0.22	8.09±1.63	3.75±0.96
350	1.21±0.10	5.88±0.50	1.71±0.23	8.48±1.61	3.70±0.91

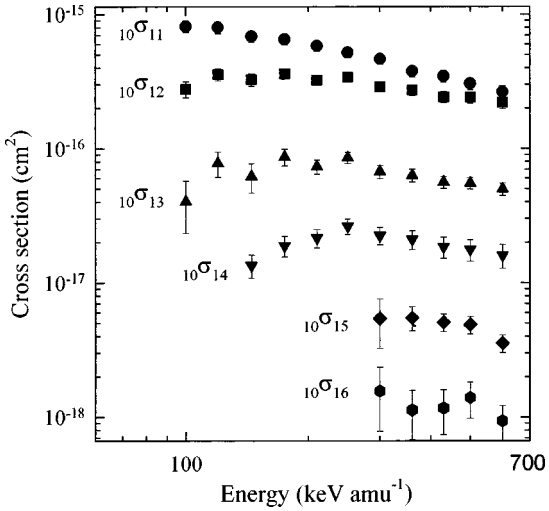

FIG. 9. Measured cross sections for pure ionization $_{10}\sigma_{1q}$ in collisions of H^+ ions with ground-state Pb atoms leading to Pb^{q+} formation.

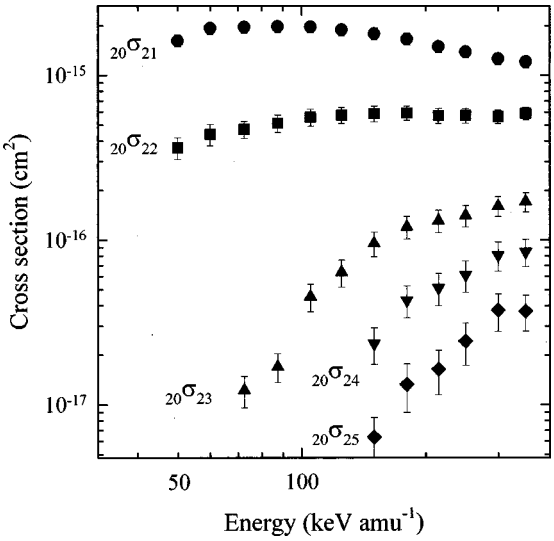

FIG. 10. Measured cross sections for pure ionization $_{20}\sigma_{2q}$ in collisions of He^{2+} ions with ground-state Pb atoms leading to Pb^{q+} formation.

converging towards values of $_{20}\sigma_{21}$ at our high-energy limit. In contrast, in a region where there is strong competition from the corresponding electron capture channels (Figs. 4 and 5), $_{20}\sigma_{23}$, $_{20}\sigma_{24}$, and $_{20}\sigma_{25}$ can be seen to be strongly energy dependent and rising towards our high-energy limit. A comparison with our results in Fig. 4 shows that transfer ionization cross sections $_{20}\sigma_{1q}$ for $q=2$, 3, 4, and 5 are only exceeded by corresponding equivelocity cross sections $_{20}\sigma_{2q}$ for pure ionization at the higher energies in the present range.

As already noted, in our previous studies of the multiple ionization of Fe, Cu, and Ga by H^+ and He^{2+} impact, we were able to describe our measured pure ionization cross sections as well as the electron capture data in terms of an independent-electron model. In our treatment of pure ionization, we assume that the probability P for the removal of an electron from a particular subshell in the process of ionization can be approximated by the expression [14]

$$P(b)=P(0)\exp(-b/R), \tag{7}$$

where b is the impact parameter and $P(0)$ and R are constants for a particular subshell. We make the simplest assumption that pure ionization primarily involves only the outermost subshells. For Pb these are the $5d$, $6s$, and $6p$ subshells which contain 13 electrons. We also assume that the individual probabilities $P(0)$ are the same for each subshell. The cross sections for pure ionization resulting in the removal of q electrons from a total of N may then be described by the expression

$$\sigma=2\pi\int_0^\infty \binom{N}{q} P(b)^q[1-P(b)]^{(N-q)} b\,db, \tag{8}$$

where $\sigma=_{10}\sigma_{1q}$ or $_{20}\sigma_{2q}$ and $\binom{N}{q}$ is the binomial coefficient.

An attempt was made to fit our measured values of $_{10}\sigma_{1q}$ or $_{20}\sigma_{2q}$ for pure ionization predicted by Eq. (8) using a weighted least-squares fit as in our previous work [4] but, in the present case, the fit with the experimental data is unsatisfactory and therefore not shown. We therefore conclude that, while this approach has been shown to be very effective in describing the pure ionization of Fe, Cu, and Ga atoms without the need to make any allowance for electron emission through Auger processes, the model appears to be too oversimplified to provide a satisfactory description of the pure ionization of Pb atoms.

V. CONCLUSION

In this work we have studied electron capture and ionization in collisions of H^+ and He^{2+} ions with ground-state Pb atoms at energies within the range 50–600 keV amu^{-1}. The separate cross sections for simple charge transfer, transfer ionization, and pure ionization leading to up to sevenfold ionized lead have been obtained. In the case of H^+ impact, pure ionization provides the dominant contributions to Pb^+, Pb^{2+}, Pb^{3+}, Pb^{4+}, Pb^{5+}, and Pb^{6+} formation over the entire energy range considered. In the case of He^{2+} impact, Pb^+ formation is dominated by pure ionization over the full energy range but Pb^{2+}, Pb^{3+}, Pb^{4+}, and Pb^{5+} production takes place mainly by transfer ionization cross sections except at the higher energies. An important feature of the present one-electron capture data is that, just as in our previous measurements on Ga, large contributions arise from transfer ionization leading to Pb^{2+} formation, which is indicative of the important role of Auger ionization processes following inner-shell electron removal. Although in our previous studies of the multiple ionization of Fe, Cu, and Ga atoms we were able to describe our observed results for both transfer ionization and pure ionization with a high degree of success using an independent-electron model, the same approach applied to Pb has been shown to be reasonably successful only in the case of one-electron capture by H^+ ions.

ACKNOWLEDGMENTS

This research forms part of a large program supported by the United Kingdom Engineering and Physical Sciences Research Council. One of us (P.C.E.McC.) has also been supported by the Department of Education, Northern Ireland.

[1] V. Shevelko and H. Tawara, *Atomic Multielectron Processes* (Springer-Verlag, Berlin, 1998).
[2] R. K. Janev, IAEA Report No. INDC(NDS)-277, Vienna, 1993 (unpublished).
[3] C. J. Patton, M. A. Bolorizahdeh, M. B. Shah, J. Geddes, and H. B. Gilbody, J. Phys. B **27**, 3695 (1994).
[4] C. J. Patton, M. B. Shah, M. A. Bolorizahdeh, J. Geddes, and H. B. Gilbody, J. Phys. B **28**, 3889 (1995).
[5] C. J. Patton, K. O. Lozhkin, M. B. Shah, J. Geddes, and H. B. Gilbody, J. Phys. B **29**, 1409 (1996).
[6] M. B. Shah, C. J. Patton, J. Geddes, and H. B. Gilbody, Nucl. Instrum. Methods Phys. Res. B **98**, 280 (1995).
[7] M. B. Shah, C. J. Patton, M. A. Bolorizahdeh, J. Geddes, and H. B. Gilbody, J. Phys. B **28**, 1821 (1995).
[8] M. B. Shah, C. J. Patton, J. Geddes, and H. B. Gilbody, in *Two-Center Effects in Ion-Atom Collisions*: *A Symposium in Honor of M. Eugene Rudd, Lincoln, NE, 1994*, edited by T. J. Gay and A. F. Starace, AIP Conf. Proc. No. **362** (AIP, New York, 1996), p. 241.
[9] K. O. Lozhkin, C. J. Patton, P. C. E. McCartney, M. Sant'anna, M. B. Shah, J. Geddes, and H. B. Gilbody, J. Phys. B **30**, 1785 (1997).
[10] J. H. McGuire, *Advances in Atomic, Molecular and Optical Physics* (Academic, New York, 1991), Vol. 29, p. 217.
[11] M. B. Shah, M. A. Bolorizadeh, C. J. Patton, and H. B. Gilbody, Meas. Sci. Technol. **7**, 709 (1996).
[12] P. C. E. McCartney, M. B. Shah, J. Geddes, and H. B. Gilbody, J. Phys. B **31**, 4821 (1998).
[13] M. B. Shah, P. McCallion, Y. Itoh, and H. B. Gilbody, J. Phys. B **25**, 3693 (1992).
[14] T. Matsuo, T. Tonuma, H. Kumagai, and H. H. Tawara, Phys. Rev. A **50**, 1178 (1994).